

Deprotonation of Zinc(II)–Water and Zinc(II)–Alcohol and Nucleophilicity of the Resultant Zinc(II) Hydroxide and Zinc(II) Alkoxide in Double-Functionalized Complexes: Theoretical Studies on Models for Hydrolytic Zinc Enzymes

Jiang Xia,[†] Yan-bo Shi,[†] Yong Zhang,^{*,†} Qiang Miao,[‡] and Wen-xia Tang^{*,†}

State Key Laboratory of Coordination Chemistry and Department of Chemistry, Nanjing University, Nanjing 210093, People's Republic of China

Received January 14, 2002

The factors governing the deprotonation ability of zinc(II)–water and zinc(II)–alcohol and nucleophilicity of the resultant zinc(II) hydroxide and zinc(II) alkoxide as complex models for zinc enzymes have been investigated through Hartree–Fock and density-functional theory methods with the 6-311++G(d,p) basis set. Our calculations showed that in these double-functionalized complexes (i.e., zinc complexes having both a zinc(II)–alcohol motif and a zinc(II)–water motif) zinc(II)–alcohol is preferred in deprotonation over zinc(II)–water (i.e., zinc(II)–alcohol has a much lower pK_a than zinc-coordinated water in the same molecule). Natural bond orbital analysis revealed that zinc(II) alkoxides are more nucleophilic than their respective counterparts zinc(II) hydroxides. The analysis of the transition state in the transformation reaction from zinc(II) hydroxide species to zinc(II) alkoxide species indicates that zinc(II) alkoxides are the preferred deprotonated species not only thermodynamically but also kinetically. Further examination of the proposed mechanisms of the zinc(II) alkoxide-promoted transesterification path and the zinc(II) hydroxide-promoted hydrolysis path revealed the structures of the intermediates and energy diagrams in the reactions. These results, entitled double-functionalized complexes, for the first time, put a firm theoretical foundation of why the zinc(II)–alcoholic OH is a better model for hydrolytic zinc enzymes (having both stronger acidity and better nucleophilicity).

Introduction

The activation of alcoholic OH by the adjacent Lewis acid, mainly Zn(II) to yield metal-bound alkoxide, accompanied by the consequent nucleophilic attack toward the electrophilic substrates is believed to be the crucial step in the hydrolysis of phosphates and RNA in some hydrolytic metalloenzymes.^{1–4} For example, in alkaline phosphatase the zinc(II)-activated serine(102) deprotonates and serves as an initial nucleophile to attack the phosphate to yield a phosphoseryl–enzyme intermediate, which is then attacked again by the adjacent zinc(II)-bound hydroxide to recycle the hydrolysis.^{5,6} Another

example goes to *Tetrahymena* ribozyme, in which a metal alkoxide group may also play an important role in the catalyzed transesterification of RNA.⁷

Some experimental examples of metal alkoxide-promoted ester hydrolysis were provided by Kimura^{4,8,9} and co-workers,^{10–15} establishing that the zinc(II) alkoxide is a more efficient nucleophilic species than zinc(II) hydroxide. In the

* Authors to whom correspondence should be addressed. Telephone: +86-25-3595706; fax: +86-25-3314502; e-mail: wxtang@netra.nju.edu.cn (W.-x.T.). E-mail: wish_you_good@yahoo.com.cn (Y.Z.).

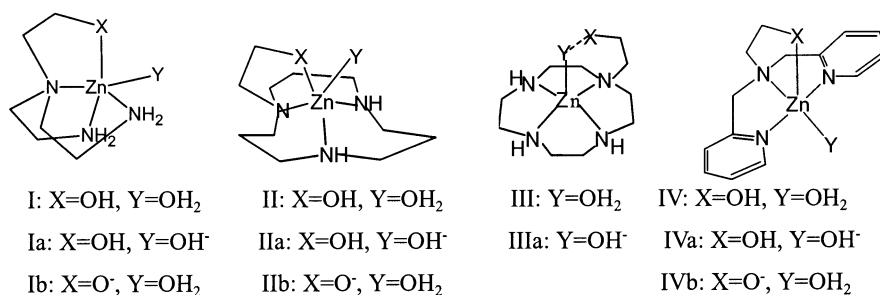
[†] State Key Laboratory of Coordination Chemistry.

[‡] Department of Chemistry.

- (1) Vallee, B. L.; Auld, D. S. *Acc. Chem. Res.* **1993**, *26*, 543.
- (2) Lipscomb, W. N.; Strater, N. *Chem. Rev.* **1996**, *96*, 2396.
- (3) Strater, N.; Lipscomb, W. N.; Klabunde, T.; Krebs, B. *Angew. Chem., Int. Ed. Engl.* **1996**, *35*, 2339.
- (4) Kimura, E.; Kikuta, E. *J. Biol. Inorg. Chem.* **2000**, *5*, 139.

- (5) Kim, E. E.; Wyckoff, H. W. *J. Mol. Biol.* **1991**, *218*, 449.
- (6) Coleman, J. E. *Ann. Rev. Biophys. Biomol. Struct.* **1992**, *21*, 441.
- (7) Steitz, T. A.; Steitz, J. A. *Proc. Natl. Acad. Sci. U.S.A.* **1993**, *90*, 6498.
- (8) Koike, T.; Kajitani, S.; Nakamura, I.; Kimura, E.; Shiro, M. *J. Am. Chem. Soc.* **1995**, *117*, 1210.
- (9) Kimura, E.; Nakamura, I.; Koike, T.; Shionoya, M.; Kodama, Y.; Ikeda, T.; Shiro, M. *J. Am. Chem. Soc.* **1994**, *116*, 4764.
- (10) Kady, I. O.; Tan, B.; Ho, Z.; Scarborough, T. *J. Chem. Soc., Chem. Commun.* **1995**, 1137.
- (11) Weijnen, J. G.; Koudijs, A.; Engbersen, J. F. *J. Org. Chem.* **1992**, *57*, 7258.
- (12) De Rosch, M. A.; Trogler, M. C. *Inorg. Chem.* **1990**, *29*, 2409.
- (13) Gellman, S. H.; Petter, R.; Breslow, R. *J. Am. Chem. Soc.* **1986**, *108*, 2388.
- (14) Sigman, D. S.; Jorgensen, C. T. *J. Am. Chem. Soc.* **1972**, *94*, 1724.
- (15) Xia, J.; Xu, Y.; Li, S. A.; Yu, K. B.; Tang, W. X. *Inorg. Chem.* **2001**, *40*, 2394.

Scheme 1



systematical modeling studies conducted by Kimura, Zn(II) complexes of macrocyclic polyamines with an ethoxyl-pendant (II and III) were used, and the reactivities of zinc(II) hydroxide and zinc(II) alkoxide for hydrolyzing 4-nitrophenyl acetate were compared.^{4,8,9} In a previous work, we synthesized a new zinc(II)-tripodal polyamine bearing an ethoxyl-pod complex to mimic the zinc(II)-serine motif in alkaline phosphatase and found that zinc(II)-tripodal polyamine can also be a good model for hydrolytic zinc enzymes.¹⁵ Chin compared the reactivities and mechanisms of copper(II) hydroxide and copper(II) alkoxides and found that the copper(II) alkoxide-promoted transesterification path is 2 orders of magnitude more efficient than the hydrolysis path (i.e., the metal hydroxide path).¹⁶

Theoretical approaches have been successfully applied on transition metal coordination chemistry.^{17–23} Bertini and co-workers investigated the deprotonation reaction of the Zn(II)-H₂O motif in various model systems using theoretical tools, leading to the conclusion that the p*K*_a of coordinated water in metalloprotein is indeed determined by the electronic properties of the metal complex as a whole and a reasonable order of nucleophilicity of the examined nucleophile generated by the deprotonation.²⁴ Specifically, Anders et al. have made significant contributions to the theoretical investigation of LZn-OH-catalyzed CS₂, CO₂ hydrolysis reactions, and carboxylation reactions of acetophenone with zinc(II) alkoxide/carbon dioxide systems. Their calculations showed that the methoxide in TpZn-OMe (zinc(II) alkoxide) should be a stronger nucleophile than the hydroxide in TpZn-OH in the reaction with CS₂ even in much smaller concentration.^{19–21} More recently, Anders et al. investigated the quantitative structure/reactivity relationship from the results of B3LYP/6-311+G(d) calculations on the hydration of carbon dioxide by a series of zinc complexes designed to mimic carbonic

anhydrase.^{19b} In this elegant paper, Anders and other researchers used the charge and the orbital energy of the lone pair on the nucleophilic oxygen atom derived from natural bond orbital (NBO) analysis to assess the degree of nucleophilicity of the zinc(II) hydroxide species. This method now serves as a paradigm for the analysis of nucleophilicity.^{19b}

To provide rational interpretation of the competition of zinc(II) alkoxide and zinc(II) hydroxide in both deprotonation and nucleophilic hydrolysis reactions, we herein conducted theoretical analysis on several double-functionalized complexes (i.e., zinc(II) polyamines bearing a hydroxyethyl group and a zinc(II)-water motif simultaneously), as illustrated in Scheme 1, to compare the formation and nucleophilicity of zinc(II) alkoxides and zinc(II) hydroxides. Systems I–III are well-suited for a direct comparison because all have been thoroughly investigated in previous experimental studies,^{8,9,15} while system IV contains two aromatic groups and is chosen in present calculations to evaluate the effect of the aromatic groups in present theoretical approaches. We examined the mechanisms of two carboxy ester hydrolysis paths: the zinc(II) alkoxide involved transesterification path and the zinc(II) hydroxide-promoted hydrolysis path, by optimizing and analyzing the intermediates and energy profiles. Present research provides the first thorough examination and comparison of the recently developed hydrolytic zinc enzyme models through theoretical approaches and probes the nature of the deprotonation of water/hydroxyethyl-pendant promoted by the adjacent Zn(II) ion and the two consequent nucleophilic attacks toward carboxy esters.

Computational Details

For a precise and systematic picture of the electronic properties of the studied complexes, a full geometry optimization procedure was performed on each system in the gas phase, which was followed by harmonic frequency analysis and single-point calculations. Initial geometries were obtained from crystal structures where available, and in other cases, the desired molecules were built through modification of the similar compounds with known structures. Density functional theory (DFT) method (specifically described as B3LYP, the Becke's three parameter hybrid functional using the LYP correlation functional²⁵) with the basis 6-311++g(d,p) was used throughout our calculations. The B3LYP-COSMO method³⁰ was used to evaluate the structural and energetic changes in aqueous solution as compared to the gas phase in system I as examples. The relative stabilities and energies of formation reported contain a correction for the zero-point vibrational energy. Reed et al.'s²⁹

(16) Young, M. J.; Wahnon, D.; Hynes, R. C.; Chin, J. *J. Am. Chem. Soc.* **1995**, *117*, 9441.

(17) Niu, S.; Hall, M. B. *Chem. Rev.* **2000**, *100*, 353.

(18) Kollman, P. A. *Acc. Chem. Res.* **1996**, *29*, 461.

(19) (a) Brauer, M.; Anders, E.; Sinnecker, S.; Koch, W.; Rombach, M.; Brombacher, H.; Vahrenkamp, H. *Chem. Commun.* **2000**, 647. (b) Brauer, M.; Perez-Lustres, L.; Weston, J.; Anders, E. *Inorg. Chem.* **2002**, *41*, 1454.

(20) Sinnecker, S.; Brauer, M.; Koch, W.; Anders, E. *Inorg. Chem.* **2001**, *40*, 1006.

(21) Kunert, M.; Brauer, M.; Kolbes, O.; Gorls, H.; Dinjus, E.; Anders, E. *Eur. J. Inorg. Chem.* **2000**, 1803.

(22) Sola, M.; Lledos, A.; Duran, M.; Bertran, J. *J. Am. Chem. Soc.* **2000**, *122*, 1466.

(23) Zhang, Y.; Guo, Z.; You, X. *J. Am. Chem. Soc.* **2000**, *123*, 9378.

(24) Bertini, I.; Luchinat, C.; Rosi, M.; Sgamellotti, A.; Tarantelli, F. *Inorg. Chem.* **1990**, *29*, 1460.

(25) Becke, A. D. *J. Chem. Phys.* **1993**, *98*, 5648.

Table 1. Comparison of Bond Lengths of Complex I on Different Levels of Theoretical Analysis^a

levels	HF/ 3-21G	HF/ 6-31G	HF/ 6-31G(d)	HF/ 6-31G(d,p)	HF/ 6-311G(d,p)	B3LYP/ 6-31G	B3LYP/ 6-311G(d,p)	B3LYP/ 6-311++G(d,p)
Zn–N1	2.122	2.203	2.195	2.191	2.192	2.173	2.162	2.201
Zn–N2	2.032	2.105	2.096	2.098	2.099	2.071	2.069	2.091
Zn–N3	2.030	2.104	2.097	2.099	2.102	2.071	2.070	2.092
Zn–O _{al}	1.977	2.056	2.083	2.083	2.085	2.062	2.089	2.103
Zn–O _{water}	2.064	2.132	2.147	2.144	2.132	2.129	2.123	2.181

^a All data are in Å.**Table 2.** Comparison of Electronic Energies on Different Systems and Different Levels of Calculation^a

levels	B3LYP/6-311G(d,p)// HF/6-31G	B3LYP/6-311G(d,p)// HF/6-31G(d)	B3LYP/6-311G(d,p)// HF/6-31G(d,p)	B3LYP/6-311++G(d,p)// B3LYP/6-311++G(d,p)
E_I	–2333.79433	–2333.79539	–2333.79502	–2333.8327658
E_{Ia}	–2333.49633	–2333.50554	–2333.50516	–2333.5521341
E_{Ib}	–2333.50779	–2333.50965	–2333.50891	–2333.5549563
E_{rel}^{OHb}	0.29800	0.28985	0.28986	0.28063
E_{rel}^{ORc}	0.28654	0.28574	0.28611	0.27781
energy diff	0.01146	0.00411	0.00375	0.00282

^a All data are in Hartree. ^b $E_{rel}^{OH} = E_{Ia} - E_I$, defined as the relative energy of the zinc(II) hydroxide species Ia choosing the undeprotonated species I as the reference, respectively. ^c $E_{rel}^{OR} = E_{Ib} - E_I$, the relative energy of the zinc(II) alkoxide species Ib choosing the undeprotonated species I as the reference, respectively.

NBO analysis was used to calculate changes in the atomic charges and the energy of the oxygen p lone pair. All these calculations were performed using Gaussian98²⁶ in the High Performance Computer Center of Nanjing University.

Results and Discussion

Evaluation of Levels of Calculation. To evaluate the efficiency of the different quantum chemical approaches and basis sets on optimization of the concerned systems, the structure of complex I was optimized at HF/3-21G, HF/6-31G, HF/6-31G(d), HF/6-31G(d,p), HF/6-311G(d,p), B3LYP/6-311G(d,p), and B3LYP/6-311++G(d,p) levels, and single-point energy calculation at B3LYP/6-311G(d,p) has been employed on the optimized HF/6-31G, HF/6-31G(d), and HF/6-31G(d,p) structures. Some important bond lengths have been listed in Table 1 for detailed comparison; the single-point energies at different levels are listed in Table 2.

When diffuse functions are included in 6-311G(d,p), the selected bonds of complex I elongated significantly in DFT calculation. Also, with the enlargement of the basis functions from 6-31G, 6-31G(d), and 6-31G(d,p) to 6-311++G(d,p), the energy difference between Ia and Ib decreased along the calculation approaches in Table 2. Since the inclusion of the

Table 3. Comparison of Relative Energies on Different Systems^a

	I gas phase	I ^c aqueous soln	II gas phase	III gas phase	IV gas phase
E^{OH}	168.52	289.83	180.04	181.46	175.88
E^{OR}	166.38	287.49	173.99		176.02
ΔE_{rel}^b	2.14	2.34	6.05		–0.14
pK_a		7.7	7.3	7.4	

^a All data are in kcal/mol, zero-point energy included. ^b $\Delta E_{relative} = E^{OH} - E^{OR}$. ^c The relative energies in aqueous solution were the result of single-point estimations (COSMO) using the gas-phase structures.

diffuse functions in optimization has significant effect on structural parameters, herein we used the most expensive but the most accurate B3LYP/6-311++G(d,p)//B3LYP/6-311++G(d,p) throughout our calculation.

Properties of Coordinated Water or Alcoholic OH. As shown in Table 3, all the comparisons of the relative energies involved in the deprotonation process were based on B3LYP/6-311++G(d,p)//B3LYP/6-311++G(d,p) calculations, with the results demonstrated. The relative energies are the energy values of those stationary points choosing the undeprotonated species as the reference, respectively.

The relative energy between the undeprotonated species and the deprotonated species will be a crucial indication of the deprotonation ability: the smaller the relative energy, the stronger the deprotonation ability.²⁴ The relative energy of the zinc(II) alkoxide species is lower than the corresponding zinc(II) hydroxide species in systems I and II. The result revealed that, in the two sites for deprotonation reaction, zinc(II)–alcohol has a preference in deprotonation over zinc(II)–coordinated water. On the other hand, the lower energy of zinc(II) alkoxides than that of zinc(II) hydroxides means that zinc(II) alkoxides are thermodynamically more stable than zinc(II) hydroxides. The $\Delta E_{relative}$ data, which are defined as the difference of relative energies between zinc(II) hydroxides and zinc(II) alkoxides, are positive for the model complex I and II, 2.14 and 6.05 kcal/mol, respectively. In system IV, the two sites seems to be of similar deprotonation

- (26) Frisch, M. J.; Trucks, G. W.; Schlegel, H. B.; Scuseria, G. E.; Robb, M. A.; Cheeseman, J. R.; Zakrzewski, V. G.; Montgomery, J. A., Jr.; Stratmann, R. E.; Burant, J. C.; Dapprich, S.; Millam, J. M.; Daniels, A. D.; Kudin, K. N.; Strain, M. C.; Farkas, O.; Tomasi, J.; Barone, V.; Cossi, M.; Cammi, R.; Mennucci, B.; Pomelli, C.; Adamo, C.; Clifford, S.; Ochterski, J.; Petersson, G. A.; Ayala, P. Y.; Cui, Q.; Morokuma, K.; Malick, D. K.; Rabuck, A. D.; Raghavachari, K.; Foresman, J. B.; Cioslowski, J.; Ortiz, J. V.; Stefanov, B. B.; Liu, G.; Liashenko, A.; Piskorz, P.; Komaromi, I.; Gomperts, R.; Martin, R. L.; Fox, D. J.; Keith, T.; Al-Laham, M. A.; Peng, C. Y.; Nanayakkara, A.; Gonzalez, C.; Challacombe, M.; Gill, P. M. W.; Johnson, B. G.; Chen, W.; Wong, M. W.; Andres, J. L.; Head-Gordon, M.; Replogle, E. S.; Pople, J. A. *Gaussian 98*, revision A.7; Gaussian, Inc.: Pittsburgh, PA, 1998.
- (27) Peng, C.; Ayala, P. Y.; Schlegel, H. B.; Frisch, M. J. *J. Comput. Chem.* **1996**, *17*, 49.
- (28) Peng, C.; Schlegel, H. B. *Isr. J. Chem.* **1994**, *33*, 449.
- (29) Reed, A. E.; Curtiss, L. A.; Weinhold, F. *Chem. Rev.* **1988**, *88*, 899.
- (30) Barone, V.; Cossi, W. *J. Phys. Chem. A* **1998**, *102*, 1995.

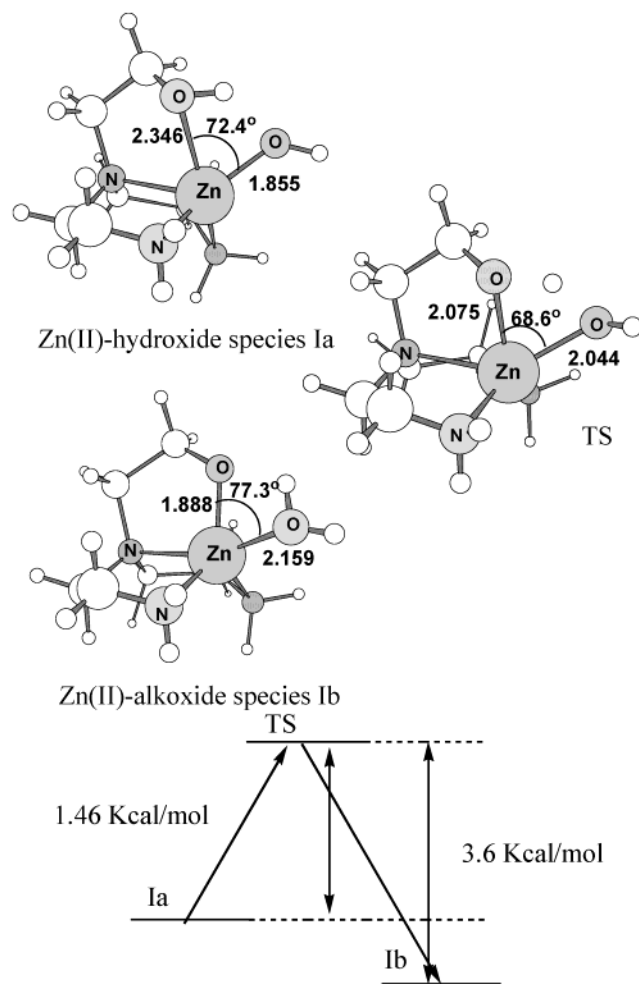


Figure 1. Optimized structures and static energies of transition state, zinc(II) alkoxide species Ib, and zinc(II) hydroxide species Ia.

nation capability. The energy difference between the zinc(II) hydroxide species IVa and the corresponding zinc(II) alkoxide species IVb is only 0.14 kcal/mol. This is probably due to the influence of aromatic groups in system IV.

For system III, according to the 2D-NMR experiment, Kimura revealed that in alkaline solution zinc(II)–water deprotonates while the alcoholic group remains uncoordinated.⁸ Our optimized structure of system III has the accordant geometry in which one water molecule occupies the apical position of a square-pyramidal geometry with the alcoholic OH forming a H-bond with the oxygen atom of water and is uncoordinated to the central Zn(II) ion, as depicted in Scheme 1. Accordingly, the zinc(II) hydroxide

species was optimized to be IIIa. Another calculation attempt with zinc(II)–water deprotonated while alcohol coordinated to Zn(II) and deprotonated leads to the same geometry as IIIa, proving IIIa to be the only stable deprotonated species, which is consistent with the proposed solution structure in the previous paper.⁸

Transition State between Zinc(II) Alkoxide and Zinc(II) Hydroxide in System I. It is usually a puzzle how to differentiate between zinc(II) alkoxide and zinc(II) hydroxide since the two monodeprotonated species in double-functionalized complexes have only one small discrepancy in the position of a hydrogen atom. However, because the two species both exist in solution because of the ES–MS results,¹⁵ we assume that the two isomers are in equilibrium. The transition state is obtained using synchronous transit-guided quasi-Newton (STQN) methods QST2,^{27,28} with zinc(II) hydroxide Ia as the first or initial structure and zinc(II) alkoxide Ib as the resultant structure. The energy profile of the interchanging reaction between zinc(II) hydroxide and zinc(II) alkoxide has been depicted in Figure 1. The energy of the transition state on the B3LYP/6-311++G(d,p) level is 3.6 kcal/mol higher than zinc(II) alkoxide and 1.46 kcal/mol higher than the zinc(II) hydroxide species. Harmonic frequency analysis of the transition state on B3LYP/6-311++G(d,p) gives the imaginary frequency of -995.232 cm^{-1} , indicating the rather significant geometric distortion. Detailed examination of the frequency mode showed that the most significant geometric change is one hydrogen atom between the hydroxide oxygen atom and the alkoxide oxygen atom. This hydrogen atom lies almost in the middle of the two oxygen atoms: $\text{H}-\text{O}_{\text{al}} = 1.218\text{ \AA}$ and $\text{H}-\text{O}_{\text{w}} = 1.220\text{ \AA}$ as compared to the data in zinc(II) hydroxide species Ia, $\text{H}-\text{O}_{\text{al}} = 0.986\text{ \AA}$ and $\text{H}-\text{O}_{\text{w}} = 1.778\text{ \AA}$ and in Ib, $\text{H}-\text{O}_{\text{al}} = 1.949\text{ \AA}$ and $\text{H}-\text{O}_{\text{w}} = 0.978\text{ \AA}$. The location of the transition state between zinc(II) hydroxide species Ia and zinc(II) alkoxide species Ib means that the two deprotonated isomers are in equilibrium. The 2.14 kcal/mol lower static energy of the zinc(II) alkoxide species Ib than of the zinc(II) hydroxide species Ia shows that thermodynamically zinc(II) alkoxide Ib is more stable than Ia; the lower activation energy in the transition from Ia to Ib means that the equilibrium biases heavily to the zinc(II) alkoxide side, resulting in a greater occupation percentage of the zinc(II) alkoxide species than the zinc(II) hydroxide species in system I.

Nucleophilicity of the Zinc(II) Alkoxides and Zinc(II) Hydroxides. The nucleophilic properties are related to the

Table 4. Comparison of Natural Charge Distribution Analysis on Different Systems

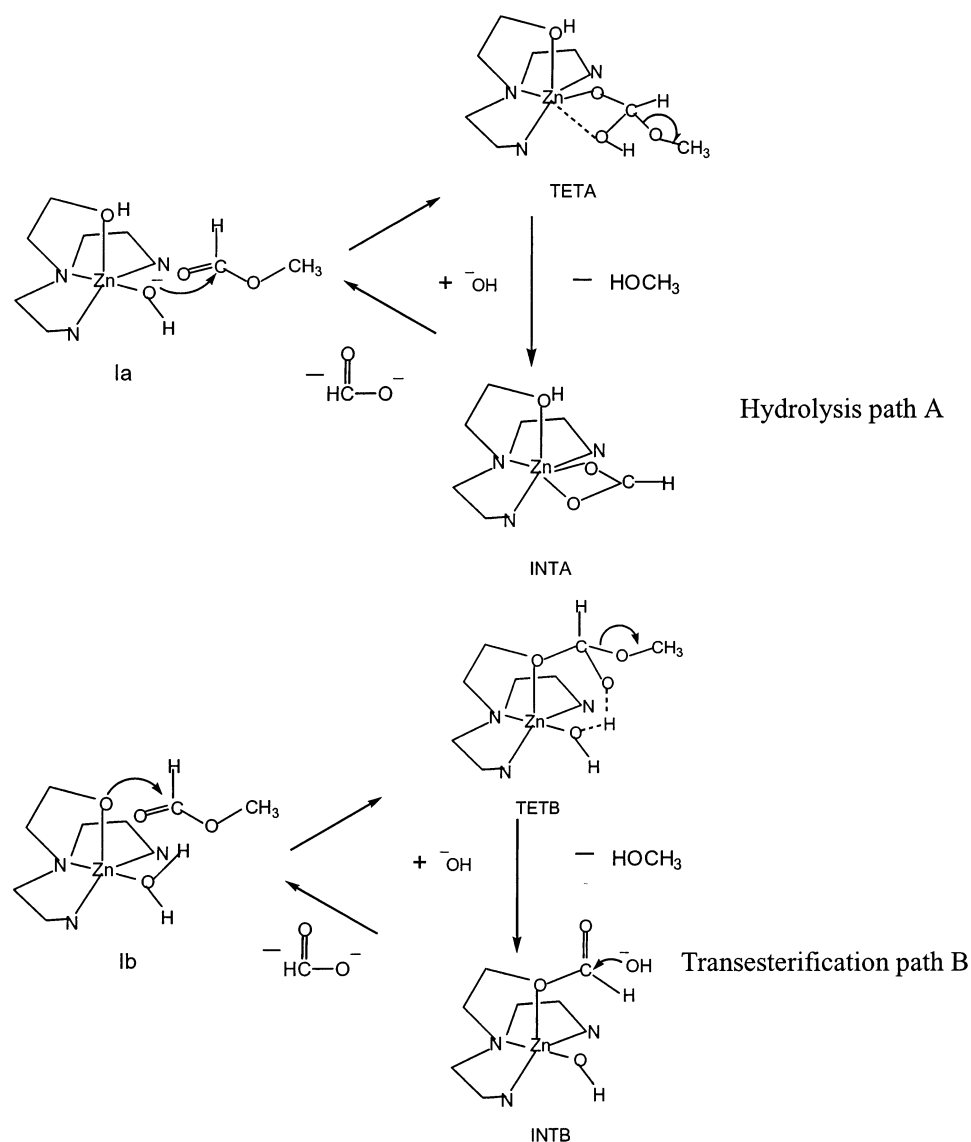
species	I		II		III	IV	
	Ia	Ib	IIa	IIb	III2	IVa	IVb
Q_{Zn}	1.623	1.628	1.626	1.625	1.617	1.651	1.640
$Q_{\text{O-water}}$	-1.316	-1.000	-1.317	-0.996	-1.307	-1.309	-0.992
$Q_{\text{(HO/H}_2\text{O)-water}}$	-0.837 (HO) _w	0.029 (H ₂ O) _w	-0.847 (HO) _w	0.006 (H ₂ O) _w	-0.852 (HO) _w	-0.851 (HO) _w	0.032 (H ₂ O) _w
$Q_{\text{O-al}}$	-0.812	-1.073	-0.804	-1.071	-0.769	-0.801	-1.064
$Q_{\text{(RO/ROH)al}}$	-0.330 (ROH) _{al}	-1.093 (RO) _{al}	-0.327 (ROH) _{al}	-1.096 (RO) _{al}	-0.329 (ROH) _{al}	-0.326 (ROH) _{al}	-1.083 (RO) _{al}
ΔQ^a		0.256		0.249			0.232

^a ΔQ is the result of the charge on nucleophilic group OH_{water} in the zinc(II) hydroxide minus the nucleophilic group charge on RO_{al} in the zinc(II) alkoxide.

Table 5. Energy of Nucleophilic Hydroxide Oxygen p Lone Pair in Deprotonated Species^a

species	I		II		III	IV ^b	
	Ia	Ib	IIa	IIb	IIIa	IVa	IVb
$E_{\text{LP-O-hydroxide}}^c$	-0.49058		-0.51210		-0.35220	-0.49625	
$E_{\text{LP-O-alkoxide}}$		-0.36650		-0.37348			-0.49920
highest E_{LP}	-0.36650		-0.37348		-0.35220	-0.49920	
nucleophilicity	0.12		0.13		0.46		
ΔE_{LP}^d	0.102		0.069			-0.00295	

^a All data are in Hartree. ^b For complex IVb, we cannot get convergence in NBO calculations on B3LYP/6-311++G(d,p). So we used the NBO calculation of IVa and IVb on HF/6-31G* for comparison. ^c $E_{\text{LP-O-hydroxide}}$, energy of nucleophilic hydroxide oxygen p lone pair in zinc(II) hydroxide species; $E_{\text{LP-O-alkoxide}}$, energy of nucleophilic alkoxide oxygen p lone pair in zinc(II) alkoxide species. ^d $\Delta E_{\text{LP}} = E_{\text{LP-O-hydroxide}} - E_{\text{LP-O-alkoxide}}$ in one system.

Scheme 2

difference in charge between the oxygen donor and the electrophilic acceptor as well as the difference in energy between the oxygen orbital involved in the formation of the new bond and the energy of the accepting orbital.^{24,19b} The more negative the charge on nucleophilic groups, the easier the substrate carrying partial positive charge will approach; the higher the energy of the oxygen p lone pair, the closer it will be to the accepting orbital of electrophilic substrates, thus favoring the formation of the covalent bond. This provides us the hint of using the charge on the specific

oxygen and the energy of the oxygen p lone pair derived from NBO analysis²⁹ as a scale of nucleophilicity for comparison, as demonstrated recently by Anders et al.^{19b} The results are listed in Tables 4 and 5.

The NBOs were conceived as a chemist's basis set that would correspond closely to the picture of localized bonds and lone pairs as basic units of molecular structures.²⁹ Both the charges on the alcoholic oxygen atom and the water oxygen atom accompanied by the overall charges of nucleophilic functional groups $(\text{HO}/\text{H}_2\text{O})_{\text{water}}$ and $(\text{RO}/\text{ROH})_{\text{al}}$ are

listed in Table 4. The overall charge of a functional group is defined as the net atomic charge with nearest atoms summed into oxygen atoms. For $(\text{HO})_{\text{water}}$, the overall group charge is the summation of the charge on the oxygen atom and that on the hydroxide hydrogen atom; for $(\text{H}_2\text{O})_{\text{water}}$, the overall group charge equals the charge on the water oxygen atom plus the charges on two water hydrogen atoms; for $(\text{ROH})_{\text{al}}$, the overall group charge means that the charge on the alcoholic oxygen atom with the charges on the adjacent alcoholic hydrogen atom and the attached carbon atom are added; for $(\text{RO})_{\text{al}}$, the overall group charge is just that on the alkoxide oxygen atom with the charge on the attached carbon atom added.

When different species of zinc(II) hydroxides and zinc(II) alkoxides within systems I, II, and IV are compared respectively, overall charges for $(\text{RO})_{\text{al}}$ in Ib, IIb, and IVb are 0.256 (-0.837 vs -1.093), 0.249 (-0.847 vs -1.096), and 0.232 (-0.851 vs -1.083) units more negative than those for $(\text{HO})_{\text{water}}$ in zinc(II) hydroxide counterparts Ia, IIa, and IVa, respectively, indicating a stronger nucleophilicity of zinc(II) alkoxides than zinc(II) hydroxides. This conclusion is well-consistent with the experimental results reported previously in the I and II-promoted carboxy ester hydrolysis process.^{9,15}

Using NBO approaches, we can easily identify the oxygen p lone pair electrons, which have the nucleophilic character. There are three lone electron pairs on water-derived hydroxide and alcohol-derived alkoxide oxygen atoms, and two lone pairs on coordinated water oxygen atoms and alcohol oxygen atoms. But we can only find one pure p-type lone pair, which is responsible for the nucleophilic attack in the respective deprotonated species. $E_{\text{LP-O-hydroxide}}$, energy of this nucleophilic hydroxide oxygen p lone pair in zinc(II) hydroxide species and $E_{\text{LP-O-alkoxide}}$, energy of this nucleophilic alkoxide oxygen p lone pair in zinc(II) alkoxide species were found to serve as another indicator of the nucleophilicity of the deprotonated species.^{19b}

$\Delta E_{\text{LP}} = E_{\text{LP-O-hydroxide}} - E_{\text{LP-O-alkoxide}}$, the energy difference between the nucleophilic hydroxide oxygen p lone pair of zinc(II) hydroxides and the nucleophilic alkoxide oxygen p lone pair of zinc(II) alkoxides are both negative in I and II in Table 5. This means that zinc(II) alkoxides have a higher nucleophilic orbital and hence higher nucleophilic ability. However, in system IV, the calculation results showed that zinc(II) hydroxide species IVa is almost the same as but a little bit more nucleophilic than its counterpart zinc(II) alkoxide species IVb (the energy difference is only 0.00295, with $E_{\text{LP-O-hydroxide}}$ higher than $E_{\text{LP-O-alkoxide}}$). Again, IV serves as an exception among all the systems, also probably because of the effect of aromatic groups. Anders et al. revealed that the zinc(II) hydroxide species of the Zn(II)-[12]aneN₄ complex has a higher nucleophilicity than the zinc(II) hydroxide species of the Zn(II)-[12]aneN₃ complex according to the 0.013 eV higher E_{LP} in the former species, which is consistent with experimental reactivity.^{19b} Our calculations give similar results according to the similarity between our systems and theirs. In systems I–III, IIIa has the highest E_{LP} , while the energy of the alkoxide oxygen p

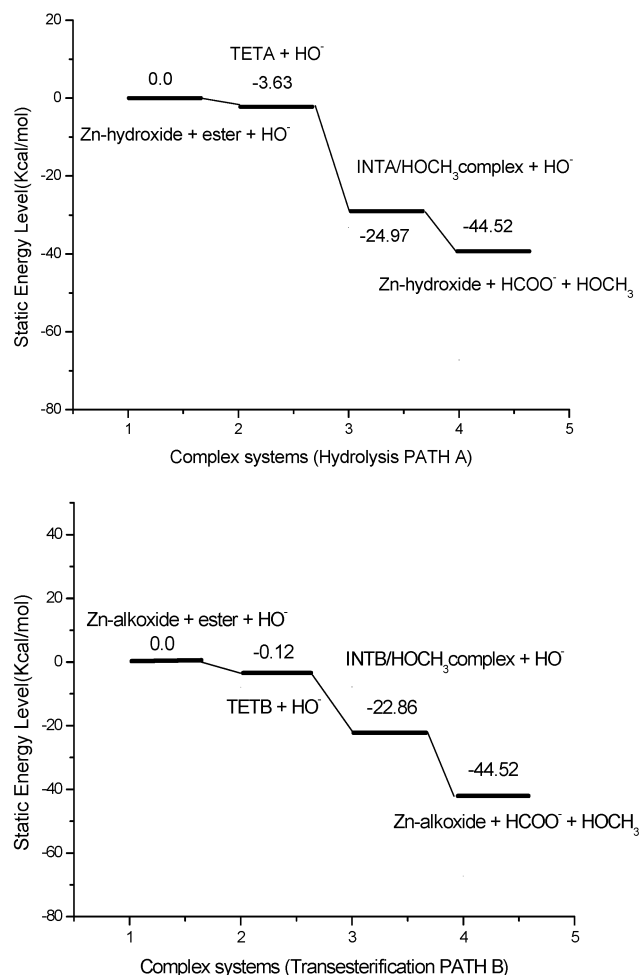


Figure 2. Energy profiles of the two different paths in Ia/Ib involving methyl formate hydrolysis. The static energies of the reactant complex systems were set as reference.

lone pair of Ib and IIb are similar. Previous experimental studies showed that system IV has a second-order rate constant of $0.46 \text{ M}^{-1} \text{ s}^{-1}$ in the hydrolysis reaction of 4-nitrophenyl acetate, while the reaction constants of I and II are $0.13 \text{ M}^{-1} \text{ s}^{-1}$ and $0.14 \text{ M}^{-1} \text{ s}^{-1}$, respectively,^{8,9,15} which is consistent with our theoretical calculations.

When the results of NBO charge distribution and orbital analysis are combined together, we concluded that by bearing more negative charge and having higher energy of the nucleophilic oxygen p lone pair, zinc(II) alkoxides are better nucleophilic reagents than zinc(II) hydroxides in systems I and II.

Solvent Effect. Because the model systems were subjected to kinetic measurements in water solution, we extended our calculations of system I to determine the properties of these systems in aqueous solution by employing the COSMO model at the B3LYP level as suggested previously.^{19b} Because of the computational demands of solution calculations at the DFT level of theory, single-point estimations of the solvation energy using the gas-phase structures were performed.^{19b} As listed in Table 3, the relative energies in aqueous solution are larger than relative energies in the gas phase in system I. But the energy difference between Ia and Ib is quite similar in aqueous solution to the energy difference

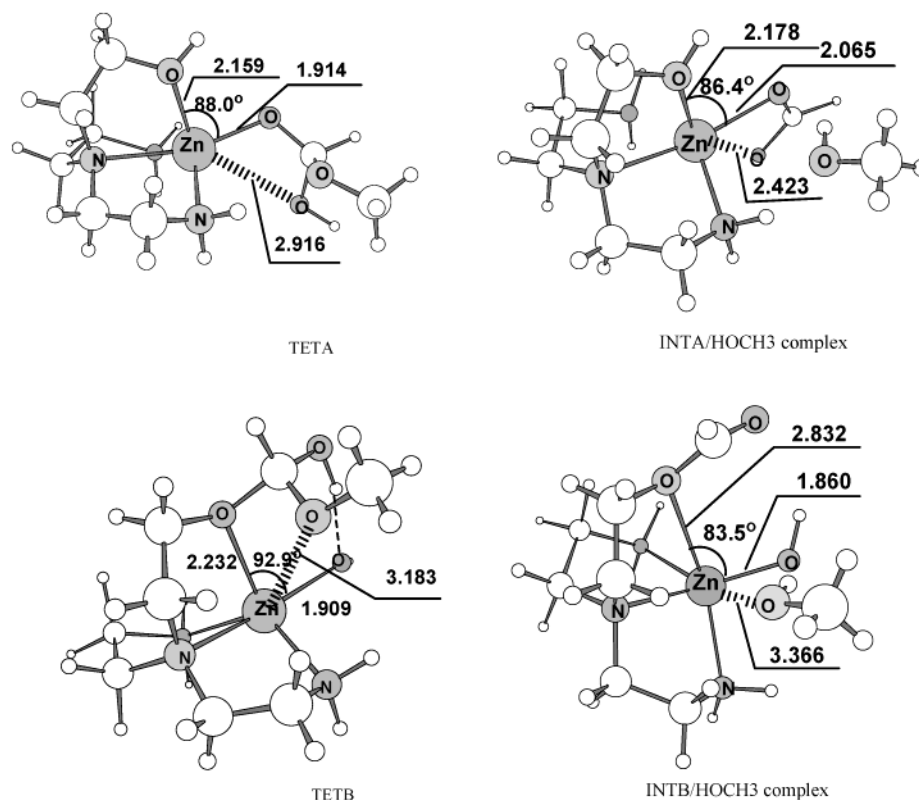


Figure 3. Disassociation of a CH_3OH molecule from the tetrahedral carbon complexes in paths A and B, displaying the optimized structures at the B3LYP/6-311++G(d,p) level of theory. TETA, TETB, the INTA/ HOCH_3 complex, and the INTB/ HOCH_3 complex are shown.

in the gas phase. Since only the energy differences between the zinc(II) hydroxide species and the zinc(II) alkoxide species are concerned in the present study (although inclusion of a solvent effect in optimization may influence structural parameters obviously), the present discussion of the calculation results in the gas phase is still useful.

Reaction Mechanisms. Hydration reaction paths of CO_2 or CS_2 catalyzed by $\text{L}_3\text{Zn(II)-OH}$ ($\text{L} = \text{imidazole, NH}_3$) have been studied by Anders et al. using theoretical approaches in which the Lipscomb and Lindskog mechanisms are compared.^{19–21} In present theoretical research work, we conduct a tentative DFT investigation on a more complicated system: the catalyst complex is Ia/Ib, while the substrate is carboxy ester methyl formate instead of CO_2 or CS_2 . Methyl formate hydrolysis processes catalyzed by zinc(II) hydroxide Ia and zinc(II) alkoxide Ib were demonstrated in Scheme 2 for comparison.

In path B, zinc(II) alkoxide involved carboxy ester hydrolysis was proposed to follow the transesterification path verified by testing and separating the covalent intermediates by NMR spectroscopy, HPLC, and synthesis previously.^{8,9,15,16} The nucleophilic attack of zinc(II) alkoxide toward the ester yields a tetrahedral intermediate TETB with a H atom shared by both the ester oxygen and the water oxygen atom. The shared hydrogen atom belonged to zinc(II)-coordinated water previously and is captured by the oxygen of tetrahedral carbon with the resultant H–O bond length of 1.588 Å. We did not find coordination number expansion in the generation of this minimum; Zn(II) remains five-coordinated, although two oxygen atoms are very near to the Zn(II) atom (3.183

and 3.334 Å). Thereafter, the carbonic tetrahedron structure TETB dissociates to release a methanol molecule to give an INTB and formate acid molecular complex called the INTB/ HOCH_3 complex. The leaving of a methanol molecule CH_3OH instead of a methanol anion CH_3O^- is verified by optimization of the structure by elongating the tetrahedral carbon–oxygen bond. The intermediate INTB is attacked by an external hydroxide anion to release a formate anion and regenerate zinc(II) alkoxide to thus recycle the hydrolysis catalysis.

In path A, zinc(II) hydroxide catalyzed methyl formate hydrolysis, TETA, the INTA/ HOCH_3 complex, and INTA are respective counterparts of TETB, the INTB/ HOCH_3 complex, and INTB in path B. However, TETA, the INTA/ HOCH_3 complex, and INTA are metal–organic complexes instead of covalent complexes. The nucleophilic attack of zinc(II) hydroxide generates TETA in which the Zn(II) atom is further coordinated to an oxygen atom belonging to the carbon tetrahedral structure with the Zn–O bond length of 2.916 Å. In this path, the coordination number of Zn(II) is expanded from five to six, which is different from the case in the transesterification path.

The covalent intermediates TETB, the INTB/ HOCH_3 complex, and INTB of the transesterification path and metal–organic intermediates TETA, the INTA/ HOCH_3 complex, and INTA of the hydrolysis path were constructed and optimized by B3LYP/6-311++G(d,p). As shown in Figure 3. Energy profiles of the two above-mentioned processes at the same computational level were plotted in Figure 2. Because we did not locate the transition states in the whole

reaction paths, it is not sufficient to conclude from present mechanism analysis which path should be dominating in aqueous solution. However, as a tentative investigation of the nucleophilic reaction paths involving zinc(II) alkoxide and zinc(II) hydroxide, the examination of tetrahedral intermediates and acyl intermediates in the transesterification path may also provide some important information about the comparison of the two paths. This topic is in further investigation.

Conclusion

The present research utilized Hartree–Fock and DFT methods to investigate the deprotonation of zinc(II)–water and zinc(II)–alcohol and nucleophilic reactivity of the resultant zinc(II) hydroxides and zinc(II) alkoxides in double-functionalized complexes. Comparison of the static energies of zinc(II) alkoxides and zinc(II) hydroxides reveals that zinc(II)–alcohol is more easily deprotonated than zinc(II)–water, indicating that a zinc(II)-coordinated alcohol has a lower pK_a than a zinc(II)-coordinated water in the same molecule. Examination of the NBO charge distribution and the energy of the nucleophilic oxygen p lone pair in deprotonated species provides the evidence of stronger nucleophilic

reactivity of zinc(II) alkoxides than zinc(II) hydroxides. We also found that the two deprotonated isomers, the zinc(II) alkoxide species Ib, and the zinc(II) hydroxide species Ia are interchangeable through a transition state easily, resulting in the equilibrium of the two isomers in solution. Further examination of the proposed mechanisms of carboxy ester hydrolysis paths promoted by the two isomers (i.e., the transesterification path by zinc(II) alkoxide and the hydrolysis path by zinc(II) hydroxide) revealed the structures of the intermediates and energy diagrams of the two paths. These results, entitled double-functionalized complexes, for the first time, clearly showed that the zinc(II)–alcoholic OH is a better model for hydrolytic zinc enzymes (having both stronger acidity and better nucleophilicity).

Acknowledgment. We are grateful to Prof. Bai Zhiping for valuable discussions and to the High Performance Computer Center of Nanjing University for computer time.

Supporting Information Available: Cartesian coordinates of INTA, INTB, the INTA/HOCH₃ complex, the INTB/HOCH₃ complex, TETA, and TETB. This material is available free of charge via the Internet at <http://pubs.acs.org>.

IC020040Z